NATURAL RADIATION DETECTION USING GAMMA RAY SPECTROMETRY

by

Nicholas Michael Nahas

A Thesis Submitted to the Faculty of the

DEPARTMENT OF NUCLEAR ENGINEERING

In Partial Fulfillment of the Requirements
For the Degree of

MASTER OF SCIENCE

In the Graduate College

THE UNIVERSITY OF ARIZONA

1 9 7 2

STATEMENT BY AUTHOR

This thesis has been submitted in partial fulfillment of requirements of an advanced degree at The University of Arizona and is deposited in the University Library to be made available to borrowers under rules of the Library.

Brief quotations from this thesis are allowable without special permission, provided that accurate acknowledgment of source is made. Requests for permission for extended quotation from or reproduction of this manuscript in whole or in part may be granted by the head of the major department or the Dean of the Graduate College when in his judgement the proposed use of the material is in the interests of scholarship. In all other instances, including reproduction of the work of art, permission must be obtained from the author.

SIGNED: Nicholas M Nakos

APPROVAL BY THESIS DIRECTOR

This thesis has been approved on the date shown below:

Morton E. Wacks

MORTON E. WACKS
Professor of Nuclear Engineering

1 July 1971
Date

ACKNOWLEDGEMENTS

The author is very grateful for the guidance and technical assistance given by Dr. Morton E. Wacks, Professor of Nuclear Engineering, and by Mr. Dennis M. Myers, a doctoral candidate, Department of Nuclear Engineering. The author would also like to thank the Engineering Experiment Station without whose financial assistance the construction of the low level counting facility could not have been completed.

TABLE OF CONTENTS

LIST OF ILLUSTRATIONS

LIST OF ILLUSTRATIONS, Continued

LIST OF TABLES

ABSTRACT

A system for the detection of naturally occurring background radiation was designed, constructed, and tested. The system consists of the breach portion of a pre-1945 naval 6-inch gun barrel used as shielding, a NaI scintillation detector for gamma ray detection, and a multichannel analyzer for data accumulation. The system is capable of measuring natural and artificial radiation levels in both solid and liquid samples. Detection limits for the naturally occurring isotopes are on the order of 1 part per million (ppm) uranium and thorium and .25 percent potassium in the sample.

Applications of the system include the monitoring of radiation levels in milk and water supplies, rock samples, and ore tailings from the various coal and copper mines in Arizona. In addition, the system provides a relatively easy and inexpensive method of gathering baseline data from various areas in the state prior to the introduction of nuclear power plants into the area.

CHAPTER 1

INTRODUCTION

Although naturally occurring radiation has always been a part of our environment, it has more recently come to the general attention of the public due to the publicity surrounding first, the detonation of nuclear devices, and secondly, the construction of nuclear power plants. Generally, radioactive nuclear species which occur naturally in our environment can be divided into three groups: (a) Primary radionuclides which are the naturally occurring nuclides and their daughters which have survived since the time when the elements were formed; (b) Cosmogenic radionuclides which are continuously formed by the interaction of cosmic-ray particles with matter; and (c) Artificial radionuclides which are introduced by human activities, such as by detonation of nuclear devices, construction and operation of nuclear power plants, and by various other scientific experiments (Lal and Suess 1968).

It is the purpose of this thesis to describe the theory, design, construction, and use of a counting facility which is capable of the measurement and identification of extremely small amounts of those naturally occurring radioactive species which emit gamma rays. Emphasis will be given to gamma ray spectrometry using a NaI scintillation detector. The basic shielding used is a portion of a 6-inch naval gun barrel made from pre-1945 steel. The pre-1945 steel is necessary to

insure low enough background radiation levels in the detector to measure these extremely small amounts of naturally occurring radioactive species.

CHAPTER 2

THEORY

Prior to discussing the operation of a low level detection device, it is necessary to understand two general concepts. These concepts are the interaction of radiation with matter and the detection of gamma rays with a scintillation detector.

The Interaction of Radiation With Matter

In order to fully understand the processes of radiation detection, it is necessary to become familiar with what takes place when various types of radiation interact with matter. This interacting radiation can take the form of alpha particles, positive or negative beta particles, gamma rays, x-rays, or bremsstrahlung. We will discuss only alpha, beta, and gamma radiation with emphasis on the gamma radiation.

Alpha particles are emitted primarily by nuclei with high atomic number. These particles are commonly emitted from naturally radioactive materials with energy between 3 and 8 Mev (Overman and Clark 1960). Due to the relatively large mass and charge of the alpha particle, (2 neutrons and 2 protons) it is very easily slowed and absorbed by any material with which it interacts. It's energy loss is due primarily to inelastic collisions with the electrons of the stopping material. Since alpha particles are monoenergetic and since they are primarily slowed by

inelastic collisions, the number-distance curve as shown in Fig. 1 is obtained. The typical range of 2 Mev alpha particles in air is only .86 cm.

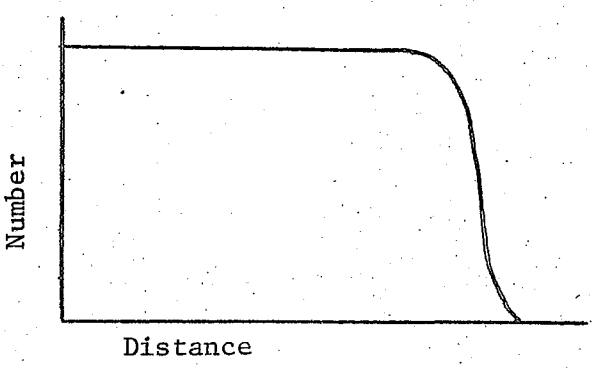

Fig. 1. Typical Number-Distance Curve for Heavy Particles (The Number of Particles Left in the Beam is Plotted Against the Distance from the Source). (Spinks and Woods 1964, p. 44)

Beta particles (electrons or positrons) interact with matter by elastic and inelastic collisions and by the emission of electromagnetic radiation. The relative importance of these methods of interaction varies with the energy of the incident particles and also, to a smaller degree, with the nature of the absorbing material. At high energy, radiation emission predominates and at low energy both elastic and inelastic scattering occur. The high energy radiation loss takes the form of bremsstrahlung which is caused when the particle passes close to the nucleus of an atom and is decelerated. This bremsstrahlung is negligible below 100 Kev and predominates at beta energies between 10 and 100 Mev. At low energies, energy is lost due to coulomb interactions with the electrons of the stopping material which produce excitation and ionization in the stopping material. For a beta particle with E Mev

energy, the ratio of the energy loss from radiation to that lost by collision is roughly given by:

$$\frac{\left(\frac{dE}{dX}\right)_{rad}}{\left(\frac{dE}{dX}\right)_{coll}} \approx \frac{EZ}{1600\ m_o c^2} \qquad (1)$$

where m_o is the rest mass of the electron in grams and Z is the atomic number of the stopping material (Spinks and Woods 1964).

Since beta particles are produced with a distribution of energies, their range is not as definitely defined as that of an alpha particle. A typical number-distance curve for beta particles is given in Fig. 2.

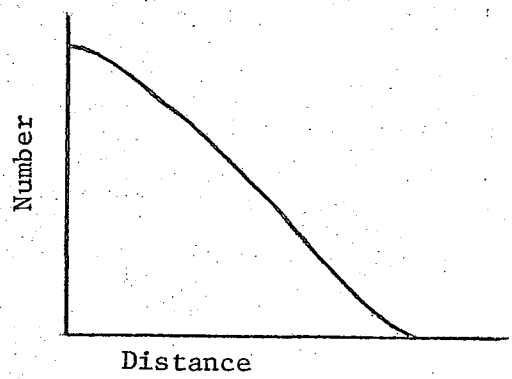

Fig. 2. Typical Number-Distance Curve for Beta Particles. (Spinks and Woods 1964, p. 19)

While charged particles tend to lose energy almost continuously through a large number of small interactions as they pass through matter, electromagnetic radiation tends to lose a relatively large amount of energy when it interacts with matter. However, not all incident photons will interact and those which do not will continue in the same direction with undiminished energy through the material. The

absorbing material will in effect reduce the number or the intensity of the photons passing through it. This reduction in intensity is given by

$$I = I_i e^{-\mu x} \tag{2}$$

x = thickness of material

I = intensity of radiation after passing through the material

I_i = initial intensity of radiation

μ = linear absorption coefficient (a direct function of the absorbing material).

The total absorption coefficient is the sum of the various partial coefficients representing the various methods of radiation interaction in matter. The three most important methods of photon interaction are the photoelectric effect, Compton effect, and pair production.

Photoelectric absorption predominates for low energy photons. In this type of interaction, the entire energy of the photon is transferred to a single atomic electron which is then ejected from the atom with the energy of the incident photon minus the binding energy of the electron in the atom. Since energy and momentum must be conserved, the electron and the ionized atom recoil in opposite directions. For this reason, the photoelectric effect is not possible with free electrons. In about 80 percent of the photoelectric processes, it is a K shell electron which is ejected provided the incident photon has energy greater than the K electron binding energy. The majority of the remaining electrons come from the L shell. The vacancy in an inner shell is

filled by one of the electrons from an outer shell. This filling of the vacancy is accompanied by the emission of secondary radiation. For materials with low atomic numbers, the binding energy of the inner electrons is relatively small and the secondary radiation will be absorbed in the immediate vicinity of the primary interaction. Conversely, materials with high atomic number will give off secondary radiation with sufficient energy for it to travel some distance before being completely absorbed. Photoelectric absorption is most probable for materials with high atomic number and for low energy photons. In addition, the photoelectric absorption shows a marked increase as the photon energy increases from just below to just above the K and L shell binding energies (Fig. 3).

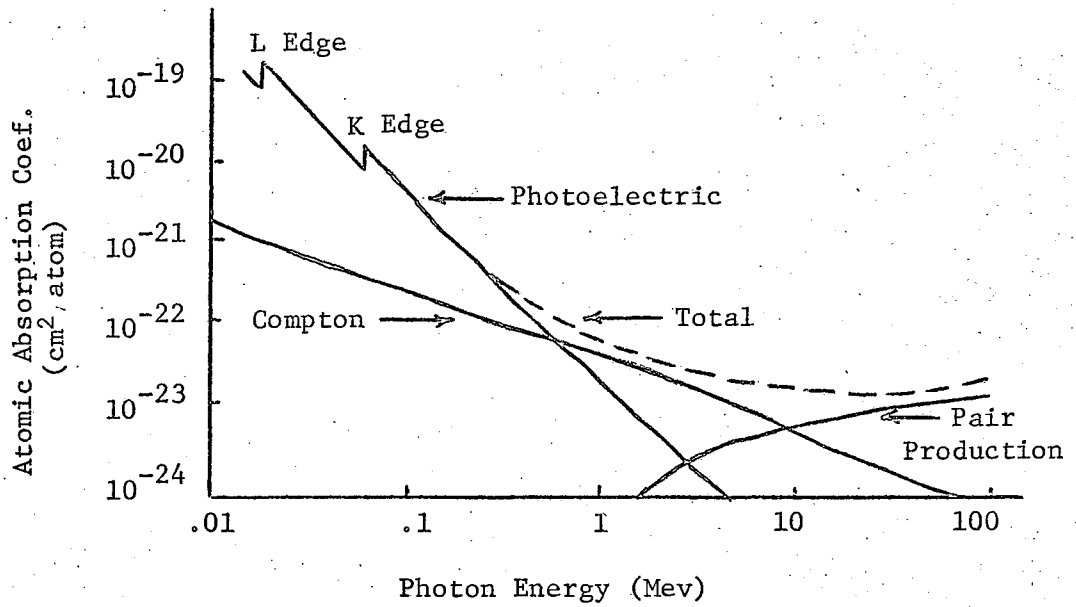

Fig. 3. Atomic Absorption Coefficients for Lead

The second possible method of photon interaction is through the Compton effect. In the Compton effect, a photon interacts with either a loosely bound or a free electron. The electron is then accelerated and the photon is deflected with reduced energy, as shown in Fig. 4.

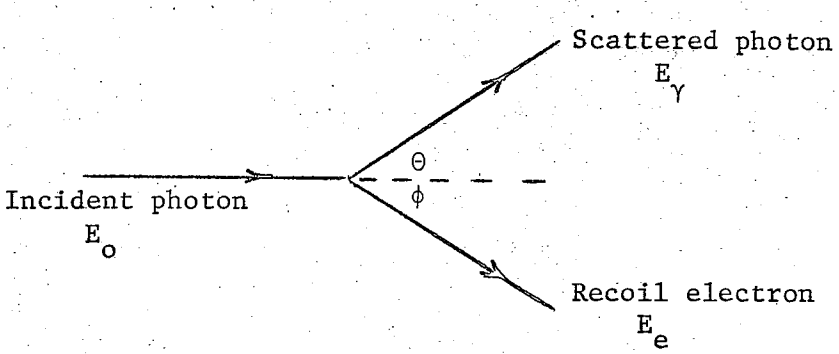

Fig. 4. The Compton Effect

The energy and momentum of the system is still conserved and is shared between the scattered photon and the recoil electron. The energy of the scattered photon is given by

$$E = \frac{E_o}{1+(E_o/m_o c^2)(1-\cos\ \Theta)} \qquad (3)$$

where $m_o c^2$ is the rest energy of the electron. The energy of the recoil electron will be equal to the difference between the energy of the incident and the scattered photon, and may have a value from zero to a maximum when the value of Θ in Eq. (3) is 180°. The Compton interaction predominates for photon energies between 1 and 5 Mev in high atomic number materials and over a much wider range for low atomic

number materials. For example, in water, the Compton effect is predominant from 30 Kev to 20 Mev (Fig. 5).

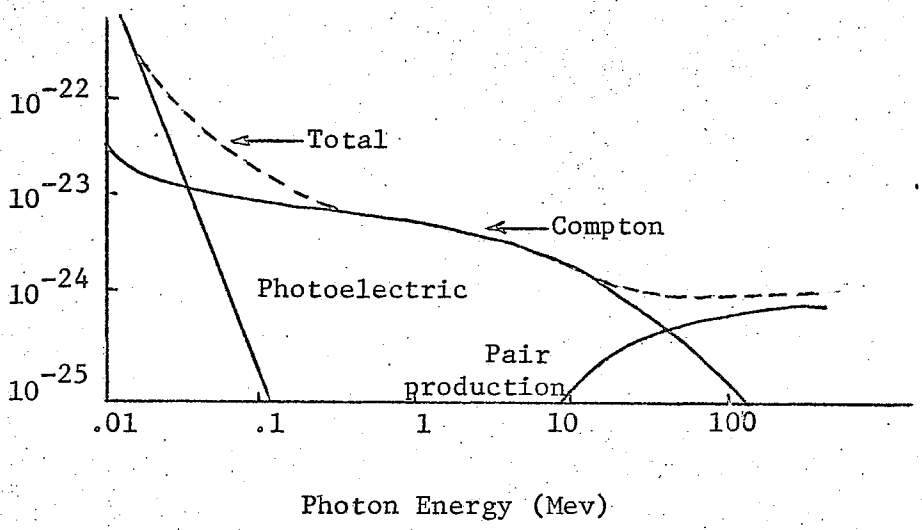

Fig. 5. Atomic Absorption Coefficients for Water

The third method of photon interaction is through pair production. In this process, the total photon energy is converted, in the vicinity of a nucleus, into an electron and a positron (Fig. 6). The energy of the photon minus the rest energy of the two particles is divided between the two recoiling particles. The positron is slowed down and eventually combines with an electron. These two particles are then replaced by two .511 Mev gamma rays which are emitted in opposite directions. These gamma rays are known as annihilation radiation and are clearly visible in the background spectrum obtained from a NaI crystal.

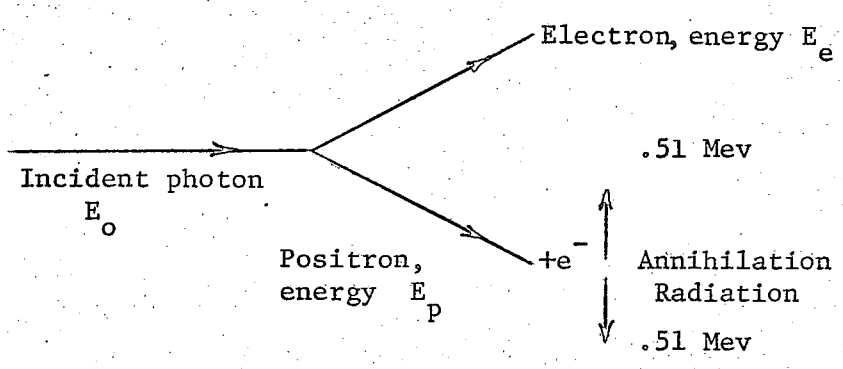

Fig. 6. Pair Production

The pair production variation for high and low atomic number material is given in Figs. 3 and 5. Pair production cannot occur below an energy of 1.02 Mev which is the minimum energy required to form the positron and electron pair (Spinks and Woods 1964).

Scintillation Detector Operation and Efficiency

With a basic understanding of the methods by which radiation interacts with matter, the types of responses a scintillation detector will give to radiation of various energies can be understood. Only the interpretation of the detector output will be discussed here and not the actual microscopic interactions. For a good explanation of these effects see Price (1964).

By way of an example, assume that a monoenergetic source of gamma radiation of .50 Mev enters into a NaI crystal detector. The absorption cross section for NaI indicates that the gamma ray will interact with the detector by both the photoelectric effect and Compton scattering with a ratio of about 6:1 in favor of the Compton scattering.

The theoretical energy distribution from these interactions will be as shown in Fig. 7. When the pulse height is measured with the NaI detector and observed on a differential pulse height analyzer, the actual spectrum is as shown by the dotted line in Fig. 7.

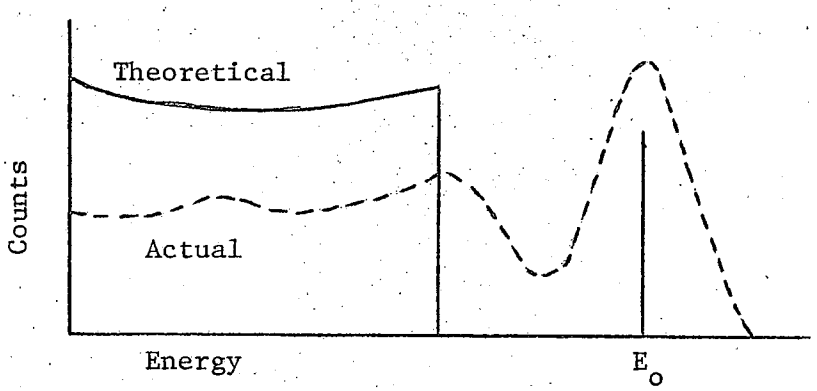

Fig. 7. Theoretical and Actual Energy Distribution for Compton and Photoelectric Interaction in a NaI Detector. (Heath 1964)

The peak resulting from total energy absorption is a characteristic of all spectra. It is also noticed that a much larger fraction of the total events actually occur in this peak than had been predicted from the Compton to total absorption ratio. This Compton to total absorption ratio is a function of the crystal size and gamma ray energy. The larger the crystal, the greater the probability that a Compton scattered gamma ray will engage in a multiple event within the crystal before escaping. If this Compton event is followed by a photoelectric event, the total energy of the gamma ray will have been absorbed, and will therefore result in a pulse height characteristic of total absorption and will not contribute to the Compton continuum.

If the energy of the incident gamma radiation is above 1.02 Mev, e.g., 1.92 Mev, the spectrum is more complicated. At this energy not only do Compton and photoelectric interactions occur but pair production is also possible. The spectrum obtained from the NaI crystal will appear as shown in Fig. 8.

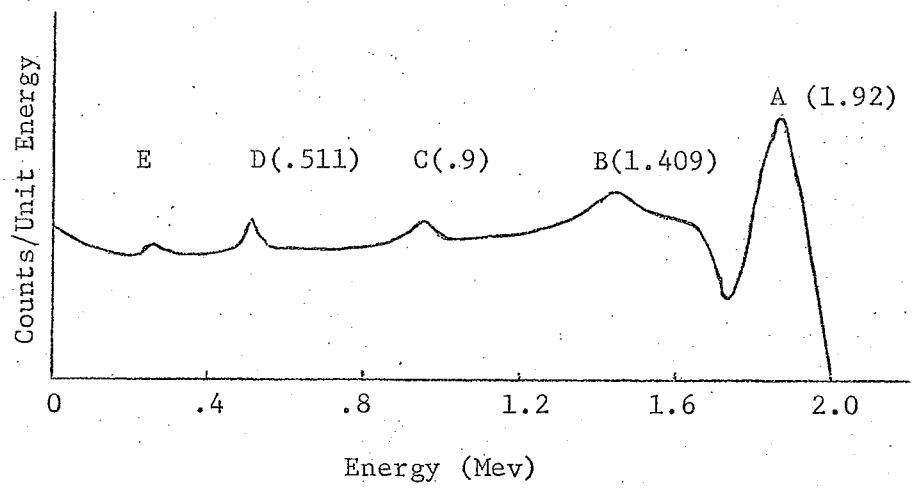

Fig. 8. Pulse Height Distribution for 1.92 Mev Gamma. (Heath 1964)

In addition to the normal total absorption peak (A), several other peaks will appear. As previously stated, it requires 1.02 Mev for pair production to occur. Any energy in excess of this will appear as kinetic energy of the positron-electron pair. Subsequent annihilation of the positron from the pair will create two .511 Mev photons. If one of the annihilation photons escapes the detector and the other is totally absorbed in the crystal by any combination of events, a peak will occur at an energy of .511 Mev less than the incident photon, or 1.409 Mev (B). This peak is known as the single escape peak. If both annihilation

photons are absorbed, the output pulse height will correspond to the total absorption peak (A). If both the photons escape the detector, a peak will appear 1.02 Mev below the total absorption peak or at .9 Mev (C). This is the double escape peak. The total result of the pair production event will then be the production of three distinct peaks, the total absorption peak (A), the single (B), and the double (C) escape peaks.

The peak at .511 Mev (D) is due to detection of the annihilation radiation resulting from pair production external to the crystal and normally in the shielding material. This peak is a major component of background radiation and is commonly referred to as the annihilation peak. The peak at (E) is the backscatter peak. As its name implies, it is caused by the detection of radiation originating in a geometrically small source which has been Compton scattered in the shielding surrounding the crystal. Instead of a backscatter peak, it is more normal to find a distributed backscatter at low energies. These distributed counts are due both to scattering of distributed sources in the shielding material and to bremsstrahlung caused by the slowing down of high energy charged particles in the shielding or sample. These charged particles may originate either internally or externally to the shield.

If it were possible to totally isolate and measure a single monoenergetic gamma source, the above peaks would be clearly visible. In actual practice, however, gamma rays of varying energies are usually being detected simultaneously thereby obscuring the distinct features of the individual photons. For this reason, the primary method used to

identify an unknown gamma emitting element is to determine the energy of the total absorption peak of that element (Heath 1964).

The efficiency of a detector is a function of several factors. These factors include the energy of the incident gamma ray, the geometry of the source, the distance of the source from the detector, and the detector size. Graphs available in Heath (1964) give the relative efficiencies of various size detectors for a point source as a function of incident gamma energy and distance of the source from the detector face. It is noted that for a low energy source directly on the crystal, the maximum efficiency is 50 percent. This is apparent since in this configuration, half of the gamma rays would be emitted in a direction away from the detector and be lost, while the other half would enter the detector and be measured. As the distance from the detector is increased, the efficiency becomes a function of the solid angle subtended by the point source on the detector face, as well as the probability of an interaction in the detector. For example, with a point gamma source of 5 Mev, 12 cm away from a 3"×3" detector, the efficiency is approximately 1 percent.

As a practical method of increasing counting efficiency for a given energy, one of two methods may be used. A "well crystal" may be used to effectively enclose the sample on three sides, thus increasing the probability of an emitted photon entering the crystal. The other possibility would be to take a larger sample and enclose the crystal on three sides with the sample (Fig. 9).

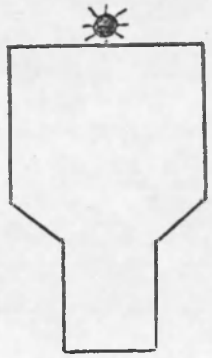

Point source
flat crystal

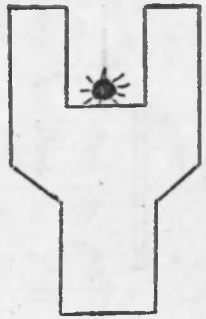

Point source
well crystal

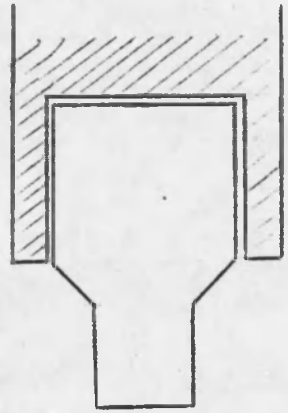

Distributed source
surrounding flat
crystal

Fig. 9. Source Geometries

Components of Natural Radiation

As previously mentioned, the three categories of natural radiation in our environment are the primary radionuclides, cosmogenic radionuclides, and artificial or man-made radionuclides.

The primary radionuclides consist of potassium-40 and the radioactive daughters found in the uranium and thorium decay series. These three elements all have half lives of greater than 10^9 years and decay by the emission of gamma rays. Potassium-40, with a 1.3×10^9 year half life comprises .0119 percent of natural potassium. It has a branched decay scheme with 89 percent going to calcium-40 by emission of a 1.3 Mev beta particle and 11 percent going to argon-40 via electron capture and emission of a 1.46 Mev gamma ray. Potassium comprises 2 to 6 percent of all granite and varying percents of other minerals depending on their location. It is therefore, present in all building materials and is clearly evident in all background spectra (Wallenberg and Smith 1964).

The presence of uranium and thorium in the environment is determined through the detection of their relatively long-lived daughters. Most of the uranium series gamma rays come from daughters of radium. The principle method of recognizing thorium is through the 2.615 Mev peak of thallium-208. The uranium series is recognized through the 1.76 Mev peak of bismuth-214. By using the relatively high energies of these daughters, it is possible to avoid the interference of the low energy Compton and backscatter photons normally encountered in the background count. In order to use these two energy peaks to

determine the uranium and thorium content, it is necessary to assume that each of the decay series is in secular equilibrium (Adams and Fryer 1964). The decay schemes for uranium and thorium are given in Figs. 10 and 11.

Due to the high energies of cosmic rays, the complete elimination of this source of background is extremely difficult. Although the cosmic rays themselves are usually not a significant contributor to the background of the detector because of their high energy (above 5 Mev), the radiation produced by the interaction of these cosmic rays with the shielding material may be significant. Cosmic rays are responsible for most, if not all, of the .511 Mev peak produced by positron annihilation. One method used to reduce cosmic activity is through the use of an anti-coincidence ring of Geiger-Muller counters. Another method is by placing the detection system underground. Argonne National Laboratory has found that by placing their detector in a large tunnel in the Chicago water system, they were able to reduce the cosmic contribution to .013 of its value at ground level. The underground count was taken below 76 meters of rock and overlay, or the equivalent of 163 meters of water (May and Martinelli 1962).

The level of artificial radioactive nuclides added to the atmosphere was greatly increased between 1954 and 1962 primarily due to nuclear weapons tests. The major radioactive elements added were ^{90}Sr, ^{137}Cs, ^{97}Zr, ^{97}Nb, ^{103}Rh, ^{85}Kr, ^{106}Rh. These nuclides may be eliminated from the background by proper shielding but may still be a contributing factor to the count rate of the sample being tested (Watt and Ramsden 1964).

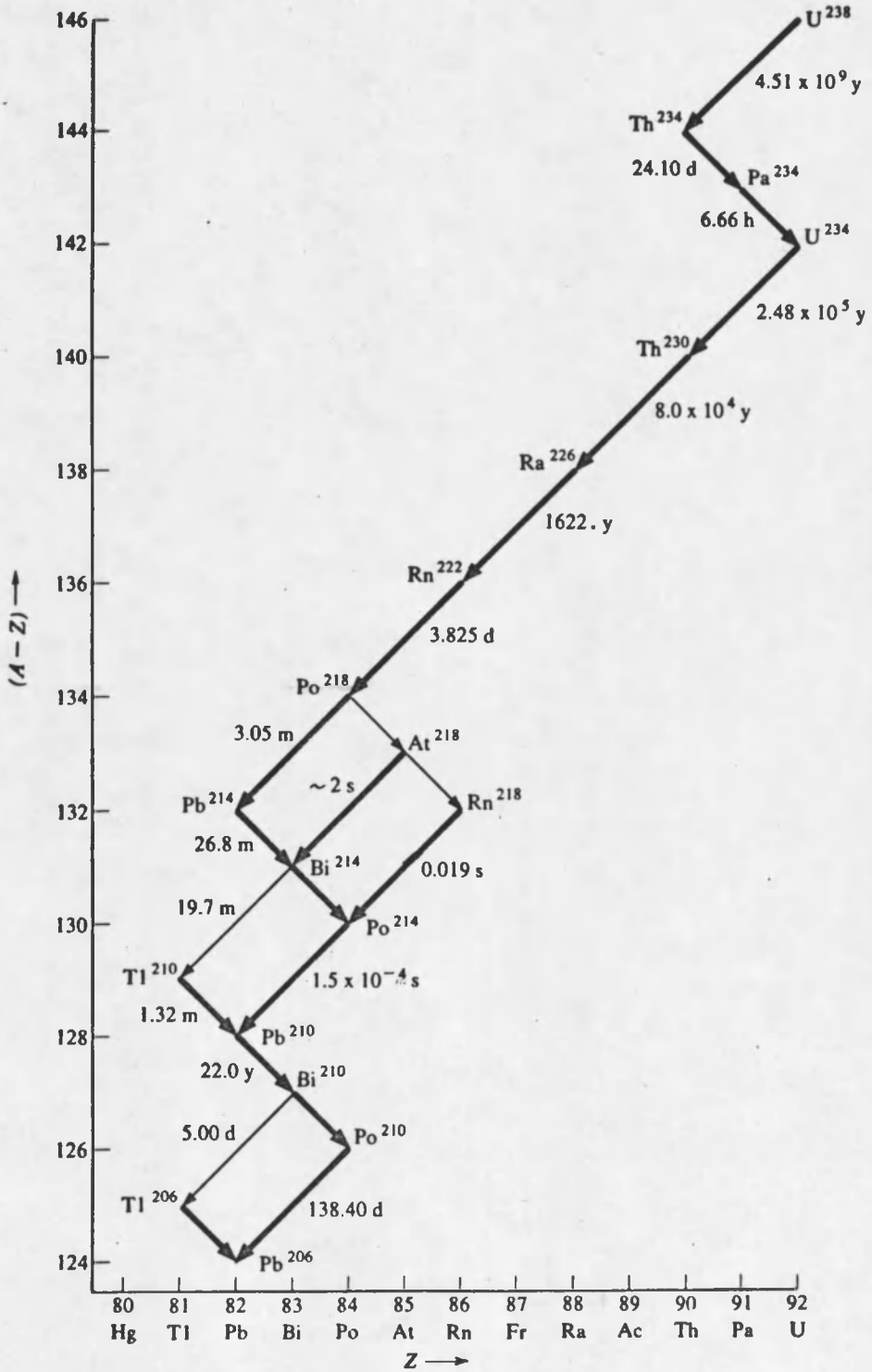

Fig. 10. Uranium Decay Scheme. (Howard 1966, p. 35)

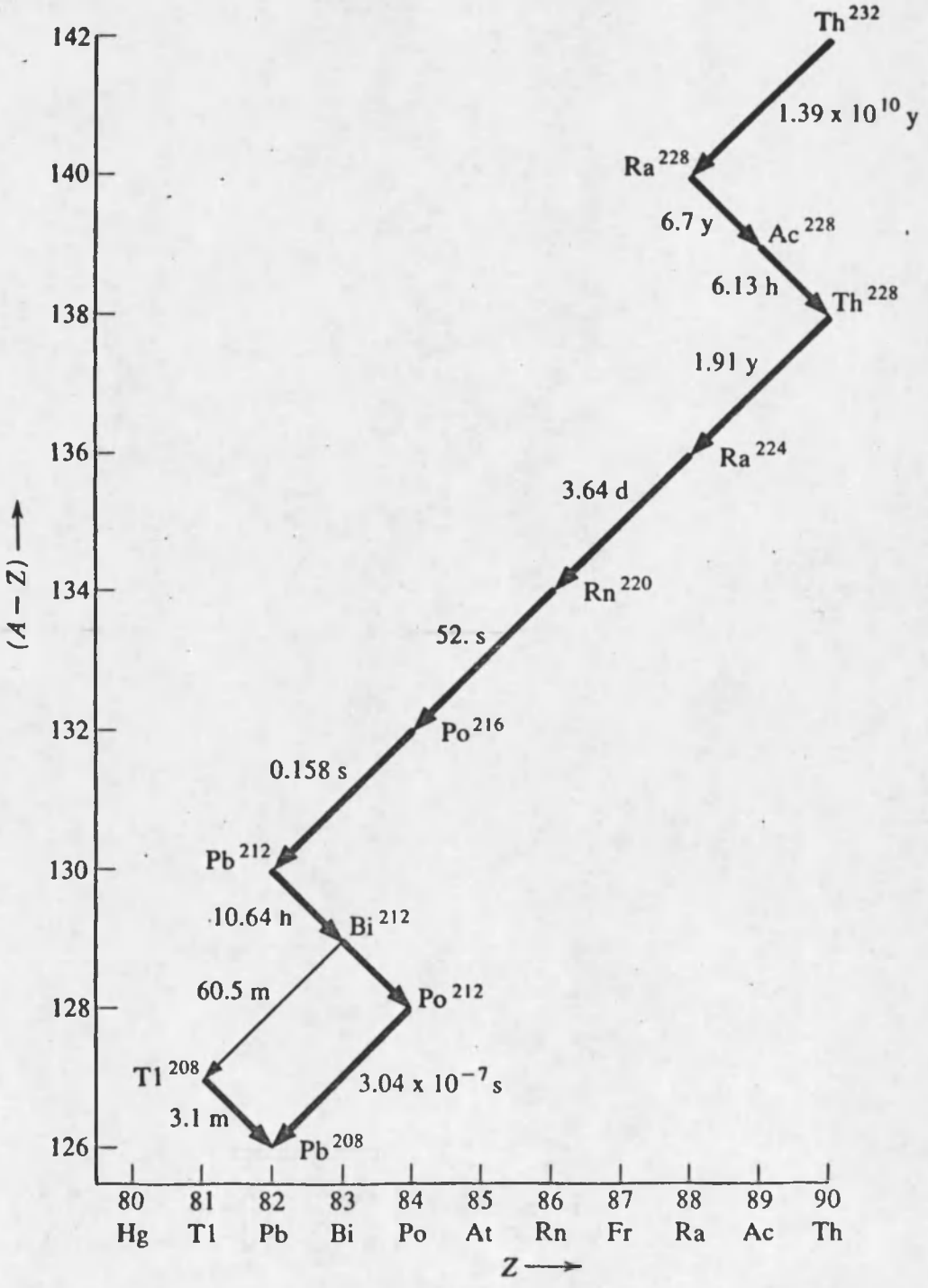

Fig. 11. Thorium Decay Scheme. (Howard 1966, p. 37)

CHAPTER 3

DESIGN AND CONSTRUCTION

In planning for the construction of a low level counting facility, several factors must be taken into consideration. These factors include location with respect to other sources of radioactivity, types of samples to be measured in the facility, type of construction material desired, and the availability of funds.

The selection of the basement location for this particular counting facility was brought about by several factors. The basement location was the farthest point from the TRIGA reactor which was available thus avoiding any interference caused by operation of the reactor at the same time a sample count might be in progress. In addition, the basement site offered three floors of building material above the detector to help reduce cosmic ray interference with count rates. Another very practical reason for the choice of the basement location was the fact that the proposed shielding material would weigh nearly two tons and it was questionable whether the upper floors would hold that weight in a concentrated area.

In an attempt to determine exactly what the background would be and if there were any noticeable variations, several background counts were taken with the unshielded detector. These readings were taken in various parts of the room, with the detector both on and off the floor. Readings were taken at night as well as during the day. Readings were

also taken with and without the reactor operating at full power. The average count rates were about 27,000 counts per minute with no appreciable variation caused by location in the room, time of the day, or operation of the TRIGA reactor. The only readily recognizable peak in the background spectrum was that from potassium-40. In all graphs, the ^{40}K peak was present, and its amplitude did not vary appreciably from one location to another within the room (Fig. 12).

Several types of material may be used in a low level counting facility. The important properties of suitable shielding materials are high attenuating power for radiation, freedom from natural or man-made radioactivity, and good scattering characteristics. Steel and lead are the two materials which have commonly been used. They are reasonably available, and meet the above requirements. Argonne National Laboratory has made extensive use of steel plates as the primary shielding material both for their small low level counting caves, and for their underground "iron room" for whole body counting (May, Corcoran, and Hess 1964).

The use of a steel gun barrel for shielding has been tried on several occasions (Vuorinen 1960 and May 1962). By using a 16-inch naval gun barrel cast in 1917, with a wall thickness of 11 inches, and a 7"×3½" NaI crystal, May (1962) obtained a count rate of 417 $\pm$ 5 counts per minute over a energy range of 30 Kev to 1.575 Mev. The spectrum obtained was extremely smooth with the only peaks in evidence being the .511 Mev annihilation peak and the 1.46 Mev ^{40}K peak (Fig. 13). The use of old (pre-1945) gun barrels is highly advisable in low level

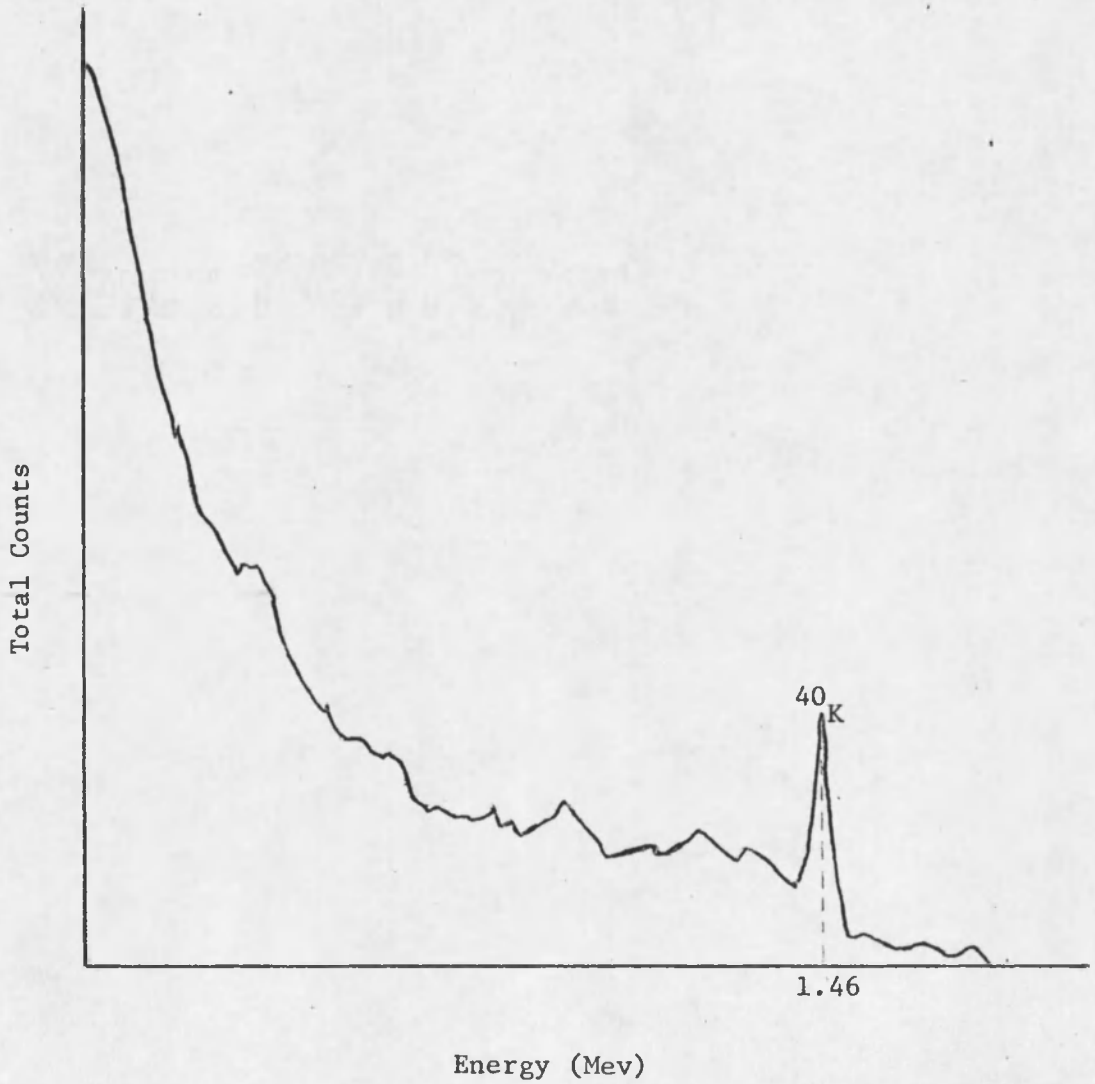

Fig. 12. Background Spectrum in Low Level Counting Laboratory with No Shielding Around Detector

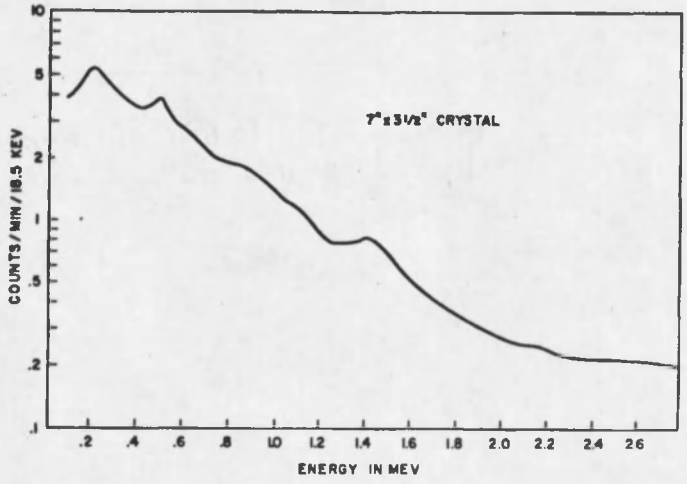

Fig. 13. Background Spectrum in 16-inch Naval Gun Barrel Shield. (May 1962)

counting experiments. These old barrels are free from contamination caused by fallout and also contamination from ^{60}Co tracers used in the monitoring of some of the more recent steel furnace operations.

Further experiments (May and Martinelli 1962) indicated that by lining either the steel plate cave or the gun barrel with 1/8 inch of low activity lead, much of the low energy count rate was eliminated (Fig. 14).

We were able to obtain an old 6-inch naval gun barrel to use as shielding for our low level counting facility. While the casting date is pre-1945, the exact date is unknown. In order to make use of the maximum wall thickness available, a four foot section was cut off the breach end of the barrel. This gave us an average wall thickness of

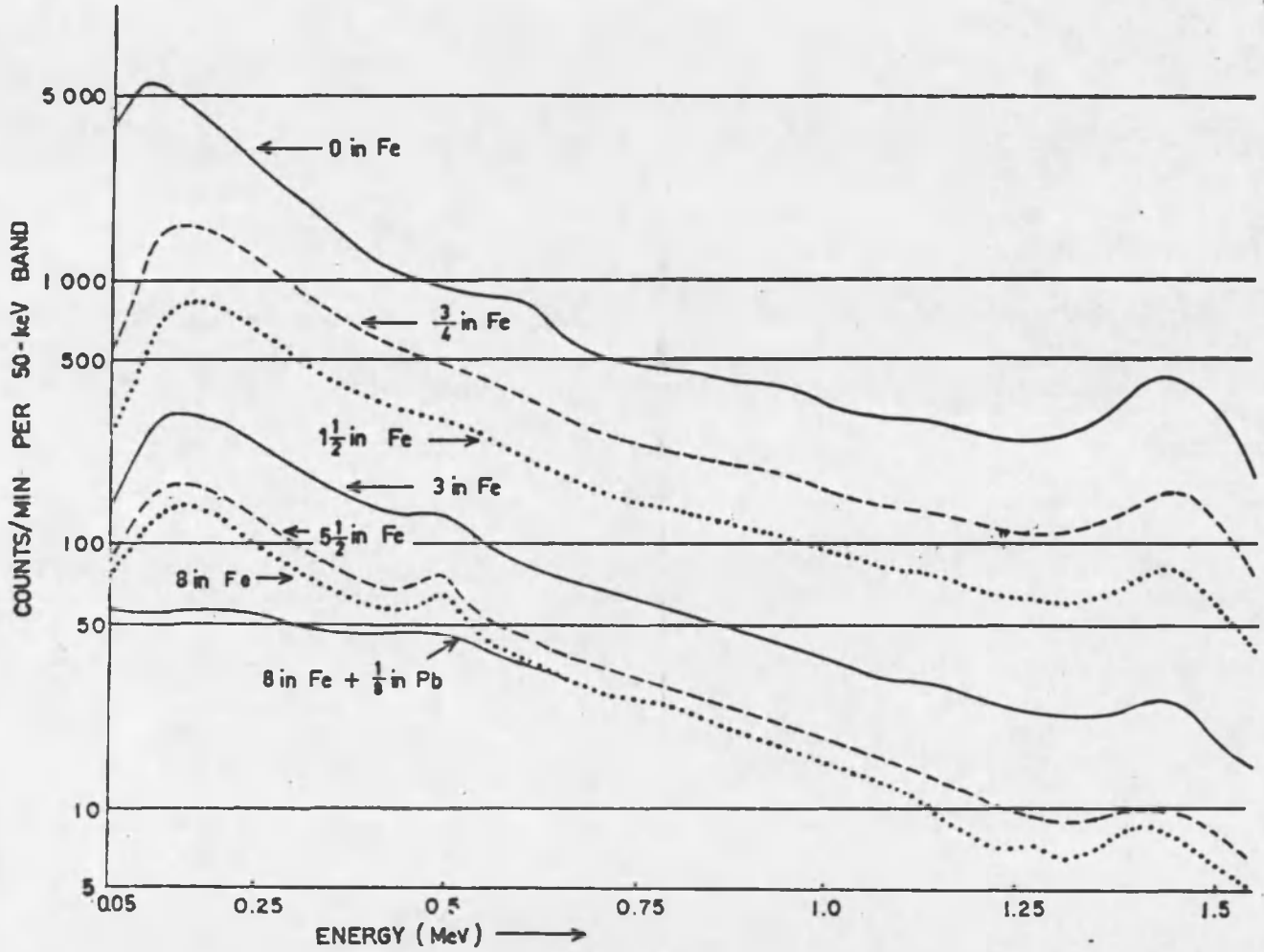

Fig. 14. Reduction in Gamma Ray Background for Various Thicknesses of Iron and Lead. (May and Martinelli 1962)

4 inches of steel with an inside diameter varying from 6½ inches to 7¼ inches (Fig. 15). The base end of the barrel is shielded with seven 1-inch pre-1945 steel plugs inserted into the breach block portion of the breach. The space around the plates was filled with low level lead which was melted and poured into place. An access hole is provided through the bottom plugs for the necessary instrument cables. These cables can be removed for repair or replacement if necessary. The top shielding consists of six 1-inch pre-1945 steel plates which slide back and forth on rollers to allow easy access for the placement of the samples to be measured. The inside of the barrel is lined with 1/8 inch of low level lead (Fig. 16).

A Harshaw 3"×3" NaI crystal is mounted upright on a plexiglas base inside the barrel. The photomultiplier tube is a 10 stage, head-on type manufactured by RCA (model 8054). The crystal and photomultiplier tube are in one self-contained unit jacketed with .032 inch aluminum. The preamplifier used was manufactured by Nuclear Chicago (model 20701). High voltage is supplied by a Fluke high voltage power supply. The recommended operating voltage to be applied to the detector is +1100 volts. Readout capability is provided by a Nuclear Data 128 channel multichannel analyzer with both paper tape and x-y plot printout capability. An external amplifier is required because of the electronic characteristics of the preamplifier being utilized (Fig. 17).

In order to provide the widest possible application, the detection device has the capability of counting both solid and liquid samples in any quantity up to one liter. A small sample may be counted

Fig. 15. Four Foot Section of 6-inch Naval Gun Barrel

Fig. 16. Completed Low Level Counting Facility

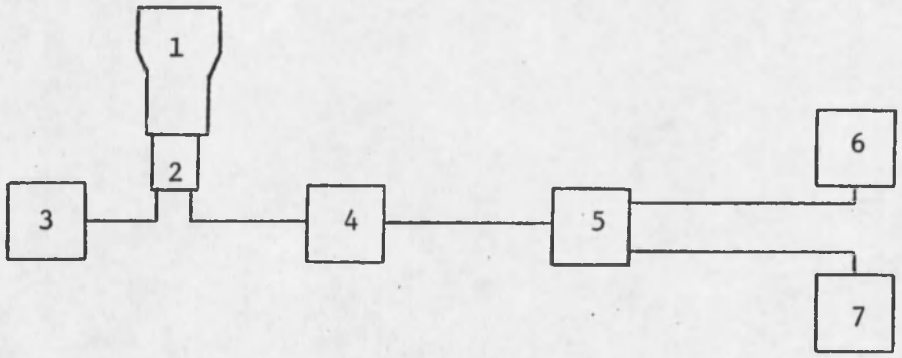

1-NaI detector with photomultiplier tube

2-Preamplifier

3-High voltage supply

4-Amplifier

5-Multichannel analyzer

6-Paper tape printout

7-X-y plotter

Fig. 17. Schematic Diagram of Scintillation Detector

by placing it in a vial and using the access tube configuration as shown in Fig. 18. In this configuration, the sample will be centered on the detector, approximately ¼ inch from the face. By removing the access tube assembly (Fig. 19), larger samples can be measured either by placing them, properly contained, directly on the crystal or, as in the case of liquid samples, by using a polyethylene reentrant cup. These cups are so constructed that a one liter sample will give one inch of coverage on all sides of the crystal (Fig. 20).

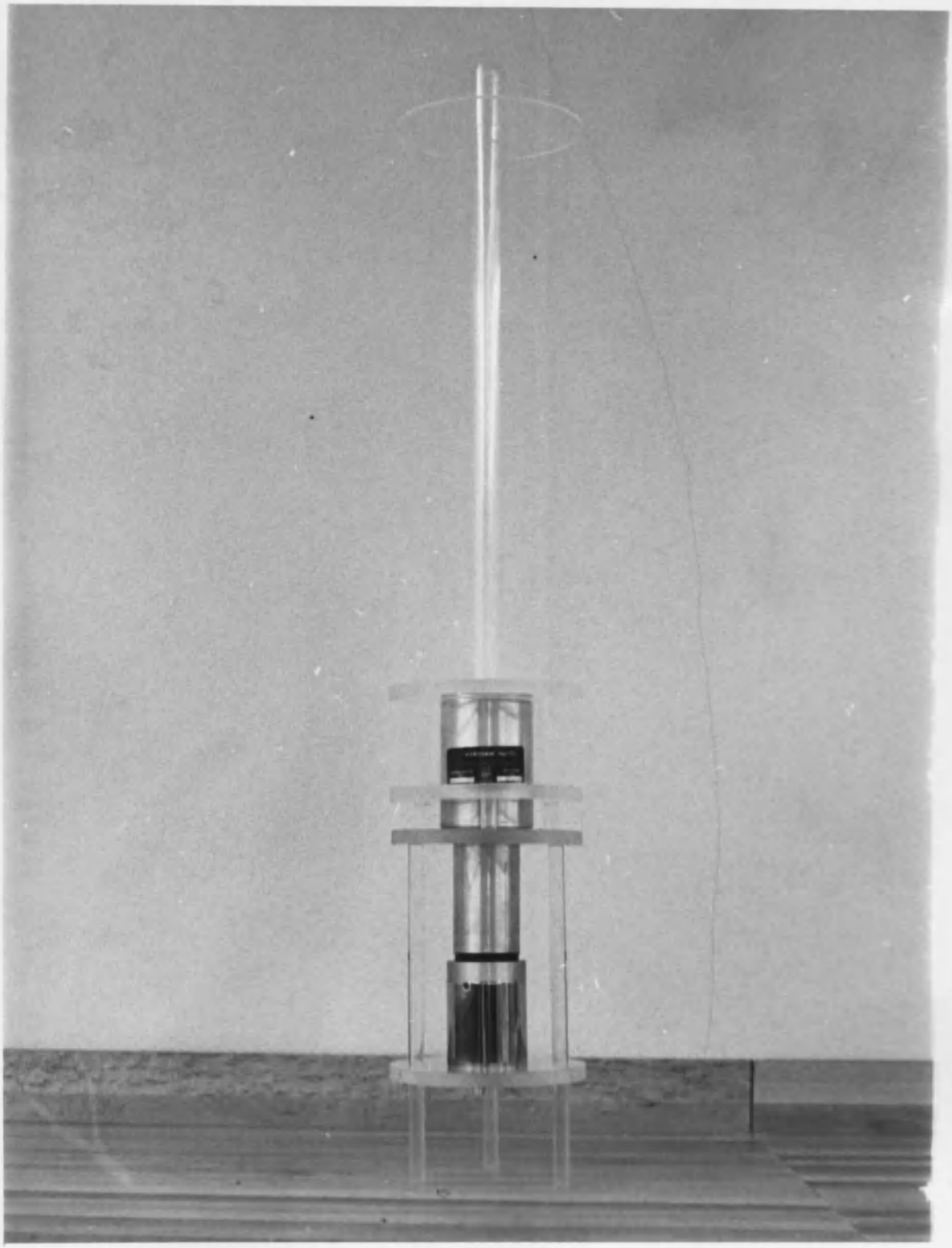

Fig. 18. Detector with Access Tube Assembly for Small Samples

Fig. 19. Detector with Access Tube Removed

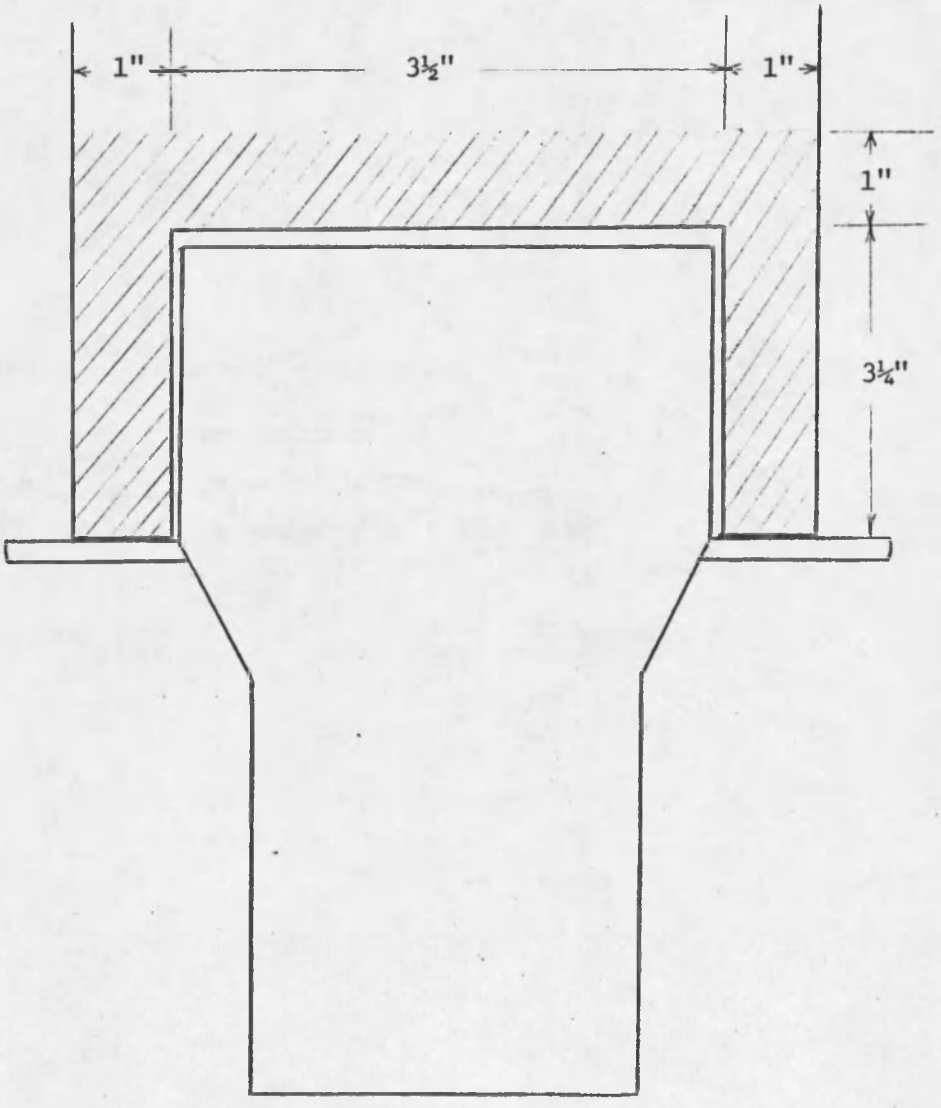

Fig. 20. Reentrant Cup Dimensions

CHAPTER 4

CALIBRATION AND OPERATION

In order to get an accurate representation of the desired background spectrum in the detection device, incoming energy from gamma rays up to and including the 2.62 Mev peak from ^{208}Tl must be measured. Therefore, for the initial background measurements, the .662 Mev peak from a ^{137}Cs standard was placed in channel 24 and the 1.33 Mev peak from a ^{60}Co standard was placed in channel 53. These settings provided an energy range from 110 Kev to 3.0 Mev with a gain per channel of 23 Kev. Preliminary measurements, before the lead liner was added to the gun barrel gave a count of 364 counts per minute over this range. After the lead liner was added, the count rate dropped to 243 counts per minute. The observed spectrum from a 17 hour count compared favorably with similar long background counts taken by Wallenberg and Smith (1964). The only definite features of the spectrum are the .511 Mev peak (channel 16) caused by the annihilation radiation, the ^{40}K peak (channel 54-58), a very weak ^{208}Tl peak (channel 104-108), and the backscatter effects at low energies caused by interactions in the shielding (Fig. 21).

The reproducibility of the background count rate based on statistical considerations of radioactive decay gives a standard deviation of $\pm$ 3 counts per minute. The count rate of 243 counts per minute has varied by $\pm$ 8. When the statistical variance of the timing device and the occasional partial loss of memory of the analyzer in one or two

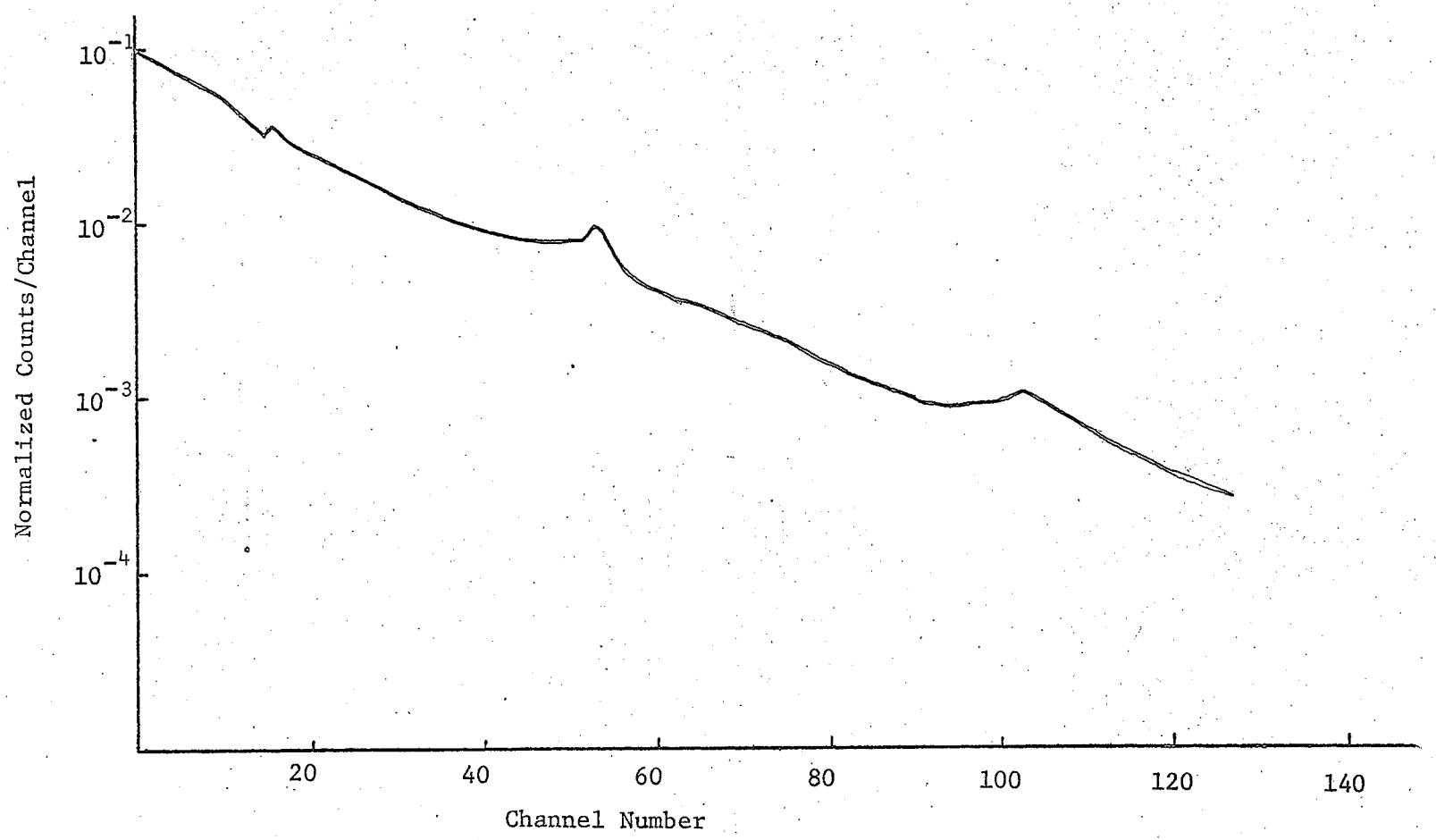

Fig. 21. Normalized Background Spectrum (17 Hour Count)

channels on long background counts are taken into consideration, the variation of less than three standard deviations in the background indicates that there are no significant random sources contributing to the background. The lack of any unaccounted for peaks in the observed spectrum would indicate that there is no detectable amount of local contamination in the detection device which would hinder the counting of low activity samples.

In order to demonstrate the operation of the counting facility, samples of various materials were counted. Water samples taken from the Brandenberg Reservoir located just west of Kingman in Oatman, Arizona, and from the Indian Health Center in northeastern Arizona, were used for the liquid samples. For solid samples, crushed Basaltic Andesite rock and crushed coal were used. The rock was borrowed from the Geochronology Department of the University of Arizona, and the coal came from Black Mesa mine in northeastern Arizona. The reentrant cup was used for the rock. There was insufficient coal to fill the liter cup so it was placed in a container directly on top of the crystal.

By observing the spectra of the two solid samples, it was possible to determine the presence of various naturally occurring isotopes of the uranium and thorium decay schemes as well as ^{40}K. At the present time, there are no standard uranium or thorium sources available in the proper geometry for use in determining the concentrations of each isotope in the solid samples. Therefore, the quantity of a given isotope can only be determined on a comparative basis. Tables 1 and 2 list the observed peaks in each of the solid samples. An independent analysis (Leventhal 1971) of the rock and coal samples indicate

TABLE 1

Observed Peaks in Coal Sample*

Channels in Peak	Isotope Observed	Energy (Mev)	Decay Series	Counts/min in Peak	Background Counts/min in Peak
32-36	^{211}Po	.89	U	18.1	11.0
41-43	^{211}Po	1.06	U	6.7	4.7
53-59	^{40}K	1.46	-	12.4	9.3
69-71	^{214}Bi	1.76	U	2.2	1.1
85-87	^{212}Bi	2.2	Th	1.4	1.0
104-109	^{208}Tl	2.62	Th	2.6	1.7

*371.6 Counts per Minute for 1318 Minutes from 110 Kev to 3.0 Mev

TABLE 2

Observed Peaks in Basaltic Andesite Rock*

Channels in Peak	Isotope Observed	Energy (Mev)	Decay Series	Counts/min in Peak	Background Counts/min in Peak
19-21	^{220}Rn	.54	Th	201	18
32-36	^{211}Po	.89	U	179	4.7
53-59	^{40}K	1.46	-	190	9.3
69-71	^{214}Bi	1.76	U	17.4	1.1
85-87	^{212}Bi	2.2	Th	9.6	1.0
104-109	^{208}Tl	2.62	Th	18.3	1.7

*3668 Counts/min for 60 Minutes from 110 Kev to 3.0 Mev.

the presence of approximately 12 ppm thorium, 3 ppm uranium, and 1 percent potassium in the rock and 12 ppm thorium, 2 ppm uranium and an unknown amount of potassium in the coal.

Standards of known concentrations of potassium were prepared in order to determine concentration of potassium in unknown water samples (Table 3). Potassium concentration in μ gms/gm of standard is plotted as a function of counts per minute in Fig. 22. A liter portion of the sample was counted using the reentrant cup in an identical geometry to that used for the calculation of the standards. The total counts in the potassium peaks of each water sample were almost identical to the total count in the background spectrum. In addition, there were no peaks which would indicate the presence of either the uranium or thorium decay schemes.

TABLE 3

Potassium Standards for Liquid Samples

µgms Potassium/gm of Liquid Sample	Time Counted (Min)	Total Counts in Peak (Channel 51-59)	Counts/min in Peak	Background Counts/min in Peak
125	300	3588	11.96	11.6
600	1023	14532	14.2	11.6
2520	1186	26488	22.3	11.6
5000	180	5639	31.3	11.6

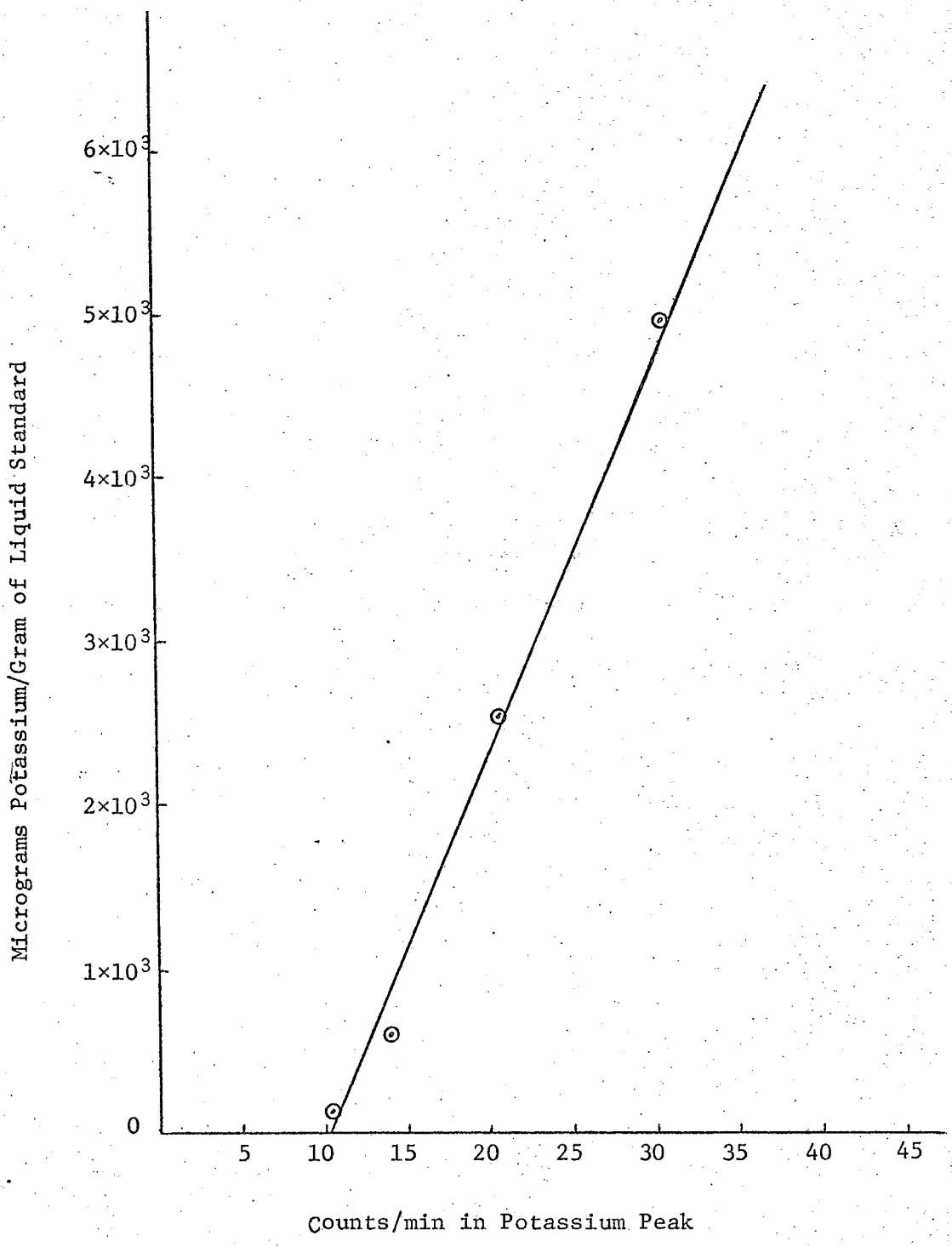

Fig. 22. Micrograms of Potassium per Gram of Liquid Standard

CHAPTER 5

CONCLUSIONS AND RECOMMENDATIONS

The usefulness of a low level radiation detection device begins to become apparent when the results of sample readings such as those in Chapter 4 are examined. With a device such as this, it is possible to determine even the smallest quantities of radioactive isotopes which may be present in our environment. The detection limits of this system appear to be on the order of 1 ppm for uranium and thorium and 125 μgrams potassium per gram of a liquid sample or .25 percent potassium in a solid sample. The flexibility which enables us to measure both solid and liquid samples is an added advantage of the above described device. In addition, the much higher count rate obtained from the rock in the reentrant cup demonstrates the desirability of using this configuration whenever possible.

This detection apparatus can be further improved by several additions and modifications. Standard samples of uranium and thorium in both solid and liquid form should be obtained. One method of obtaining standards would be to have a rock or liquid sample counted in some other facility such as Argonne National Laboratory, and use the cross calibrated results as a standard sample for this facility.

A relatively simple modification to the system would allow semiconductor detectors to be used in the same or a similar shielding configuration. The use of semiconductor detectors would enable alpha

and beta particles to be detected as well as the gamma rays now detected with the NaI crystal.

The background could be further lowered by flushing the gun barrel with CO_2 thus helping to eliminate airborne radioactivity (Brar, Nelson, and Gustafson 1967).

At some future date, nuclear power plants will undoubtedly be added to the electrical supply system of Arizona. Prior to that time, however, a thorough analysis should be made of the radioactive contents of the ground water and soil of proposed nuclear sites. These analyses will in effect give the background levels of radiation present in the area prior to the introduction of nuclear power plants. From a public relations, as well as an ecological point of view, this information is essential as a basis for the formulation of the plant safety records in future years. While there are numerous techniques by which this information might be obtained, the above described detection facility provides an easy, inexpensive, rapid, and accurate method of making these background measurements.

REFERENCES

Adams, J. A. S., and Fryer, G. E., "Portable Gamma Spectrometer for Field Determination of Thorium, Uranium, and Potassium," The Natural Radiation Environment, Chicago: University of Chicago Press, 1964, pp. 577-596.

Brar, S. S., Nelson, D. M., and Gustafson, P. F., "A New Shield for Gamma-Ray Spectrometry," Int. Journal of Applied Radiation and Isotopes, Vol. 18, 1967, pp. 261-265.

Heath, R. L., Scintillation Spectrometry Gamma-Ray Spectrum Catalogue, Vol. 1, 2nd Edition, 1964.

Howard, Robert A., Nuclear Physics, Belmont, California: Wadsworth Publishing Company, Inc., 1966.

Lal, D., and Suess, Hans E., "The Radioactivity of the Atmosphere and Hydrosphere," Annual Review of Nuclear Science, 18, 1968, pp. 407-434.

Leventhal, Joel, Department of Geochronology, University of Arizona, Personal Communication, 1971.

May, Harold A., "Neutron Production in Massive Shields and Effects Upon the Low-Energy Gamma-Ray Background," Argonne National Laboratory Radiological Physics Division Semiannual Report, January through June 1962, ANL 6646, pp. 50-65.

May, Harold A., Corcoran, John B., and Hess, Paul, "An Underground Laboratory for High Sensitivity Gamma-Ray Counting," Argonne National Laboratory Radiological Physics Division Annual Report, July 1963 through June 1964, ANL 6938, pp. 194-205.

May, Harold A., and Martinelli, Leonidas D., "Sodium Iodide Systems: Optimum Crystal Dimensions and Origin of Background," Reprinted from "Whole Body Counting," International Atomic Energy Agency, Vienna, 1962.

Overman, Ralph T., and Clark, Herbert M., Radioisotope Techniques, New York: McGraw-Hill Book Company, 1960.

Price, William J., Nuclear Radiation Detection, 2nd Edition, New York: McGraw-Hill Book Company, 1964.

Spinks, J. W. T., and Woods, R. J., An Introduction to Radiation Chemistry, New York: John Wiley & Sons, Inc., 1964.

Vuorinen, P. U., "Effective Background Shield for Low Activity Measurements," Review of Scientific Instruments, Vol. 31, 1960, pp. 573-574.

Wallenberg, Harold A., and Smith, Alan R., "Studies in Terrestrial Gamma Radiation," The Natural Radiation Environment, Chicago: University of Chicago Press, 1964, pp. 513-566.

Watt, D. E., and Ramsden, D., High Sensitivity Counting Techniques, New York: The Macmillan Company, 1964.

6519